ZIBELINE INTERNATIONAL PUBLISHING

ISSN: 1024-1752 (Print)

CODEN: JERDFO

Journal of Mechanical Engineering Research & Developments (JMERD)

DOI: *http://doi.org/10.26480/jmerd.03.2019.55.61*

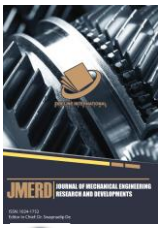

CrossMark

RESEARCH ARTICLE

APPLYING PHOTOELASTICITY WITH OPTICAL MAGNIFICATION METHOD TO INCREASE PRECISION OF DETERMINING FRINGE ORDER UNDER MONOCHROMATIC LIGHT

M.B.H Sitorus[1]*, Melvin Emil Simanjuntak[1], Agus Sigit Pramono[2], Henry Lumbantoruan[3], Udur January Hutabarat[1], B. Ginting[1], Piktor Tarigan[1], Teng Sutrisno[4]

[1]Department of Mechanical Engineering, Politeknik Negeri Medan, Jl. Almamater No.1, Kampus USU, Medan 20155
[2]Department of Mechanical Engineering, FTI ITS, Jl. A. R. Hakim, Sukolilo – Surabaya 60111
[3]Department of Electronics Engineering, Politeknik Negeri Medan, Jl. Almamater No.1, Kampus USU, Medan 20155
[4]Mechanical Engineering Department, Petra Christian University, Jl. Siwalankerto No.121-131, Siwalankerto, Wonocolo, Surabaya, Jawa Timur 60236
**Corresponding Author Email: bsm4rk@gmail.com*

ARTICLE DETAILS

Article History:

Received 01 March 2019
Accepted 10 April 2019
Available online 16 April 2019

ABSTRACT

Photoelasticity method was used to measure strain and stress fields to address the precision problem of determining fringe order of loading and cracking and notch areas. In this study, microscope was used as an additional tool in a photoelastic device for magnification of isochromatic fringe size. An experimental method was used by utilizing optical system and reflective polariscope. A simple compression tool was designed to provide a compression load on the solid disk-shaped specimens. Isochromatic fringe field was observed in the loading zone for different loading and captured image based on the following conditions: 9x, 15x and 20x without magnification and with magnification using SLR type Nikon camera Serie D3000. The image was processed using OpenCV software while C + + was used to produce clearer isochromatic fringe pattern formed on the surface of the specimen in the determination of the maximum fringe order observed. The average of additional fringe could be obtained as the optical magnification result. Data was analyzed using Finite Element Analysis Software. The result showed an increasing trend in fringe order with increasing levels of optical magnification. Its maximum value was obtained on20x optical zoom, which was 2-order fringe.

KEYWORDS

Photoelasticity, fringe order, loading zone, monochromatic light, image processing

1.INTRODUCTION

The application of the photoelasticity method to determine experimental stress is not new. The experimental method of photoelasticity is a well-known optical method which has been widely used for stress analysis in the mechanical components such as stress field near a crack tip, stress of Screw- and CementRetained Implant Prostheses, bi-material notch stress, and other applications [1-4]. Photoelasticity is an optical, non-contact technique used for field stress analysis which provides information related to principal stress difference (isochromatic) and principal stress direction (isoclinic) in the form of fringe contours. In the early days of its development, quantitative isoclinic (θc) and isochromatic (N) data were obtained only at the fringe contours.

Intensity can be divided into two stages: model preparation and fringe analysis [5]. Experimental results using the standard photoelasticity method needs a certain amount of fringe for precision in the measurement of strain field. The problem in determining the ring order often occurs in a loading zone or at an area where the load occurs because in that area amount of fringe formed is prodigious which makes it difficult in in determining the precise fringe order [6]. It leads to an error in determining fringe order in that area which known as 'dense error' [7].

Various methods and approach had been employed to minimize this problem, among of them by using of certain algorithms to process the image captured from experimental results, also by repairing the usage of optical elements, such as the utilization of additional optical tools to certain magnifying area on investigating specimen. Some researchers are using a phase unwrapping method to solve the problem because photoelastic testing produces wrapped isoclinic and isochromatic phase maps which must be unwrapped [8,9].

Digital photoelasticity also encourages the development of photoelasticity in determining experimental stress [10,11]. Some research uses techniques, such as RGB photoelasticity, digital image analyzing around isotropic point, such as three Fringe Photoelasticity (TPF), phase shifting and combination of phase shifting and RGB [12-16]. A researcher introduced optical magnifying where unwrapping technology is done by combining optical magnification with shearing stress to evaluate local stress information [17]. In that experiment, conventional optical element composition was used to analyze photoelasticity by using an epoxy disc model with 0,06 m and 0,005 m in thickness that compress diametrically. The CCD three-color detector was used to record the photoelastic RGB digital image. The ratio factor of the first image magnifying to the original is 2,5, and ratio factor of second image magnifying to the first image magnifying is 2.2. Validation is done by comparing experimental data and theoretical data had shown that there are good unconformities, where the

relative error between experimental data and theoretical data was less than 4%. A previous researcher has introduced a new approach in isoclinic unwrapping to determine fringe order value and isoclinic angle that free from noise in every pixel at all [18]. The fundamental weakness of this method is when isochromatic value obtained from experiment only has a small wave, smoothing does not produce a significant effect and the absolute error is 0.05 fringe order. It also involves a complicated analysis and one needs to wait a long time to obtain results. A recent scholar used photoelasticity method for optical magnification and image processing of stress-strain field to accelerate failure analysis of the material [19]. Optical magnification was done by using a combination of loupe (glass magnifier) and camera telescope. The total magnification wasn't described in that experiment.

This study aims to get a clear image of the fringe in the loading zone, in particular to show the tendency of dense fringe. It utilized microscope to get optical magnification at the loading zone, which is then combined with image processing to clarify the captured image.

2. METHODOLOGY

This is an experimental research using an optical system. A microscope was used to obtain an optical magnification 9x, 15x and 20x from the original specimen.

2.1 Materials

A device was used to make a simple compression load (Figure 1) and the research object was a solid disc made from urethane rubber with a diameter (D) = 60 mm, and thickness (h) = 6 mm shown in Figure 1. The rubber material has a modulus of elasticity (E) = 3.1 MPa, Poisson's ratio v = 0.46 and a voltage fringe value, f = 1.81 N / cm fringes. The choice of a disk shape specimen is to ensure static loading conditions on a rotating object that is in contact with other elements.

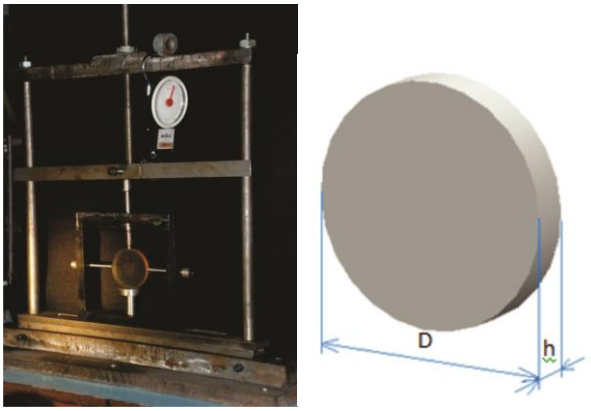

(a) (b)

Figure 1: Loading device (a) and specimen design (b)

2.2 Experimental Setup

In this experiment, the research variable was load Pi and object magnification M as an independent variable used to determine the fringe order N relate directly to a difference of principal stress (σ_1-σ_2).

(a) (b)

Figure 2: (a) A microscope attached on polariscope (b) A microscope attached on polariscope with the camera

The set-up of Reflection Polariscope 030-Series is shown in Figure 2 (a). The microscope is placed in front of the analyzer lens. To record optical magnification images, an ocular lens position and an adaptor camera attached to the camera body. The complete set up of microscope and image capturing device, i.e. Nikon SLR is shown in Figure 2 (b).

2.3 Photoelastic behaviors

The photoelasticity method requires the utilization of two types of optical element, i.e. polariser and the wave plate. Photoelastic model behavior like a temporary wave plate, relative retardation δ (relative angular phase shift) was used to change the refractive index on material loading. Relative retardation occurred among refractive light component in the principal direction and was directly proportional to the principal stress, which was perpendicular to the light propagation. The third principal stress σ3 was parallel with the direction of light propagation so that it did not affect relative retardation.

Relative retardation expressed by:

$$\delta_{12} = \frac{2\pi.h.c}{\lambda} \cdot (\sigma_1 - \sigma_2)$$

$$\delta_{23} = \frac{2\pi.h.c}{\lambda} \cdot (\sigma_2 - \sigma_3)$$

$$\delta_{31} = \frac{2\pi.h.c}{\lambda} \cdot (\sigma_3 - \sigma_1) \text{ [20]} \quad (1)$$

With h = material thickness
λ = light wavelength

In photoelastic application, brewster is usually not used directly, result in relative retardation in case of plane stress expressed by:

$$\sigma_1 - \sigma_2 = \frac{N.f_\sigma}{h} \text{ [20]} \quad (2)$$

Where

$N = \frac{\delta}{2\pi}$ = no dimension number

$f_\sigma = \frac{\lambda}{c}$ = value of material fringe in lb/in or N/m

The difference of principal stress in two-dimensional model may be determined if N (fringe order) can be measured and material fringe value fσ may be determined by calibration. The actual function of polariscope determines the value of N in every note of the object.

In the model with the linear elastic property, the difference of principal strain (ε1-ε2) may also be measured by determining fringe order N. Stress-strain relationship in the case of two-dimensional plane stress is:

$$\varepsilon_1 = \frac{1}{E}(\sigma_1 - \nu\sigma_2) \qquad \varepsilon_2 = \frac{1}{E}(\sigma_2 - \nu\sigma_1) \quad (3)$$

so that:

$$\varepsilon_1 - \varepsilon_2 = \frac{1+\nu}{E}(\sigma_1 - \sigma_2) \text{ [20]} \quad (4)$$

By substituting equation (2):

$$\varepsilon_1 - \varepsilon_2 = \frac{1+\nu}{E} \cdot \frac{N.f_\sigma}{h} = f.N$$

where

$f_\varepsilon = \frac{1+\nu}{E} f_\sigma$, so that:

$$\varepsilon_1 - \varepsilon_2 = \frac{N.f\varepsilon}{h} \text{ [20]} \quad (5)$$

The value of material fringe constant can be determine experimentally by using a known stress difference σ_1-σ_2 in a model made from the same material with the specimen under study by observing the relationship value of N and solving equation (2) :

$$f_\sigma = h\frac{\sigma_1 - \sigma_2}{N} \quad (6)$$

2.4 Determine fringe order

The method to determine fringe order using coating depends on the response of the coating and the accuracy needed for analysis. If the response is high (4 or more), monochromatic light may be used to get the fringe isochromatic pattern using bright and dark field. Commonly these fringes can be interpolated or extrapolated near to 0,2 fringe, with accuracy of 5% based on 4 fringes.

For fringe pattern between 2 and 4, the color pattern was produced from white light. It was essentially produced from decomposition or elimination of one or more color from the white light spectrum. The observed fringe color was produced by spectrum portion transmitted through the white light spectrum. The sequence of fringe color which was produced by increasing stress is shown in Table.1. The color produced is a function of the white light spectrum energy distribution. The sequence of color can be detected visually. We used a technic to determine fringe order precisely, where maximum fringe order is less than 2 with accuracy of 5% or less. This technic is a point by point method increase accuracy significantly in determining size of the fringe order.

Table 1: Isochromatics fringe characteristic

Color	Approximate relative retardation (nm)	Fringe order (N)	Strain (με)
Black	0	0	0
Gray	160	0.8	265
White	260	0.45	425
Pale Yellow	345	0.60	570
Orange	460	0.80	760
Dull Red	520	0.90	855
Purple	575	1.00	950
Deep Blue	620	1.08	1025
Blue Green	700	1.22	1160
Green-Yellow	800	1.39	1320
Orange	935	1.63	1550
Rose Red	1050	1.82	1730
Purple	1150	2.00	1900
Green	1350	2.35	2230
Green-Yellow	1440	2.50	2380
Red	1520	2.65	2520
Red / Green Transition	1730	3.00	2850
Green	1800	3.10	2950
Pink	2100	3.65	3470
Pink / Green Transition	2300	4.00	3800
Green	2400	4.15	3940
Type PS-1 Photoelastic Plastic, 0.080in (2 mm) thick			
f = 950 με/fringe (reflection)			

2.5 Image Processing

Image processing in this experiment is useful to obtaining a clearer the image results, especially in the isochromatic fringe pattern formed on the disc after loading disk. In this case the image processing is done by using Open CV C ++ code. The same image processing is done with different color detection rates (in the range of 0 to 100) because the resulting quality is different for each image. Image processing in this experiment is useful to

obtain a clearer image result, especially in the isochromatic fringe pattern which was formed on the disc after applying a load. Image processing was done first by inputting and determining image detection level, i.e. isochromatic image then changing it to gray image. The next step was changing the grey image to a binary image (black-white) based on the detection level and reducing it to white note. The last step was finishing of the fringe detection image and saving the image in png file.

2.6 Comparison

Data collected from the experiment are analyzed using finite element software. The result of the principal stress difference in the loading zone was compared with the result from experimental data before magnification and after magnification.

3. RESULT AND DISCUSSION

3.1 Modelling

The experimental specimen was figured and modelled using the commercial finite element software with geometrical specification and material properties as urethane rubber material with diameter 60mm, thickness 6 mm, density 1.25x10-3 kg/mm3, elasticity modulus 3.1 MPa and poisson ratio 0.46.

Numerical analysis results showed a contour of stress intensity, i.e. maximum principal stress difference and minimum principal stress difference (σ_1-σ_2) which occurred with the rate of the load from 5.04 N, 7.54 N, 10.04 N and 12.54 N as shown in Figure 3.

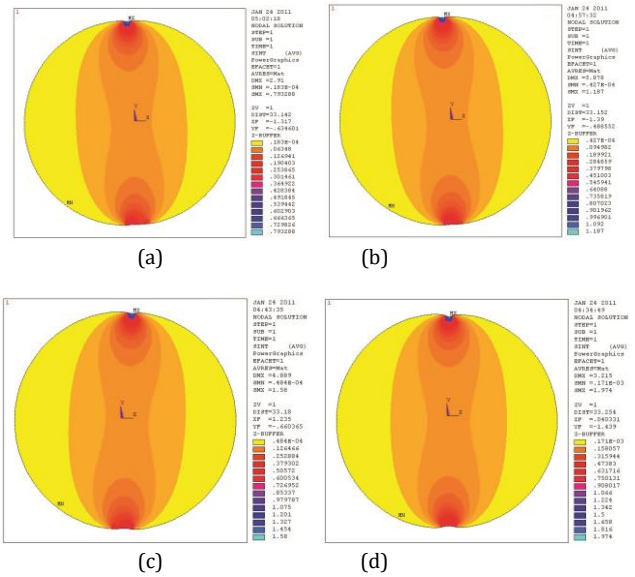

(a) (b)

(c) (d)

Figure 3: Stress intensity contour with loads for (a) 5.04 N, (b) 7.54 N (c), 10.04 N, and (d) 12.54 N

Figure 3 shows results from meshing with 1 mm length, 3407 elements and 10410 nodes. The maximum stress intensity value occurred at the loading zone, in this case in node 2 (light blue color).
All of the numerical analysis results are shown in table 2.

Table 2: The numerical analysis result data in the loading zone

No	Load (N)	Stress intensity $\sigma_1 - \sigma_2$ (MPa)
1	5.04	0.7933
2	7.54	1.1870
3	10.04	1.5800
4	12.54	1.9740

This table shows stress intensity will increase corresponding with load intensity.

3.2 Experimental Result

The experiment was conducted using monochromatic lights from the red halogen lamp to obtain bright-dark isochromatic fringe pattern to simplify the image processing. The image captured using photoelasticity method with 9x optical magnification is shown in Figure 4.

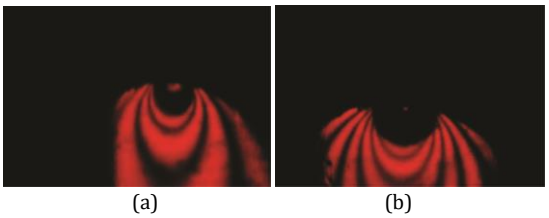

(a) (b)

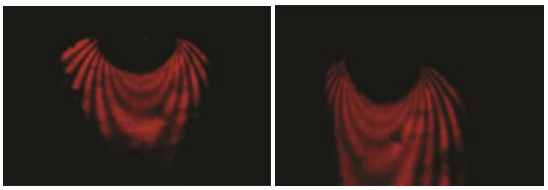

(c) (d)

Figure 4: The fringe pattern with load 5.04 N (a), 7.54 N (b), 10.04 N (c), and 12.54 (d) at magnification 9x

The result of image processing by photoelasticity method with 9x optical magnification is shown in Figure 5.

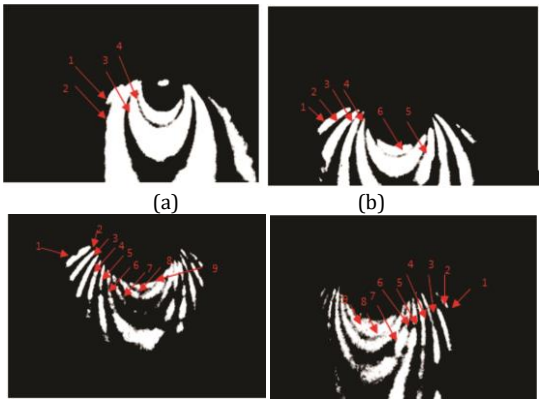

(a) (b)

(c) (d)

Figure 5: The result of image processing with load 5.04 N (a), 7.54 N (b), 10.04 N (c), and 12.54 (d) at 9x magnification

It can be seen that at the top of the specimen there is a dark pattern, hence, it is not possible to calculate the fringe in that section.

By enlarging the optical magnification at 15x and 20x optical magnification at the top of the specimen, there is also a dark pattern like in the previous enlargement image so it is not possible to calculate the fringe in the section.

It can be seen that almost all of the isochromatic fringe lines formed on the disc can be clearly observed except at the top end of the specimen, where the loading is located, and at the lower end of the disc, where the constraint is located. At that location, the order of the fringe is difficult to determine because of the proximity of the adjacent fringe orders. Therefore, it is necessary to process the image for clarity, so it is easier to calculate the fringe order and then determine the difference between maximum principle voltage and minimum principal stress from the related fringe order.

3.3 Comparing Result

Based on image processing and by using equation (2), maximum fringe order was observed in conditions respectively without optical magnification, and with9x magnification, 15x magnification, and 20x magnification as shown in Table 3.

Table 3: The maximum fringe order based on load and optical magnification

Magnification	Maximum fringe order Load (N)			
	5.04	7.54	10.04	12.54
1x	4	6	7	7
9x	4	6	9	9
15x	4	8	9	10
20x	6	8	9	11

The plot of fringe order counting graph with Magnification respectively 1x (light blue line), 9x (red line), 15x (light green line) and 20x (indigo line) based on increasing load received can be shown in Figure 6.

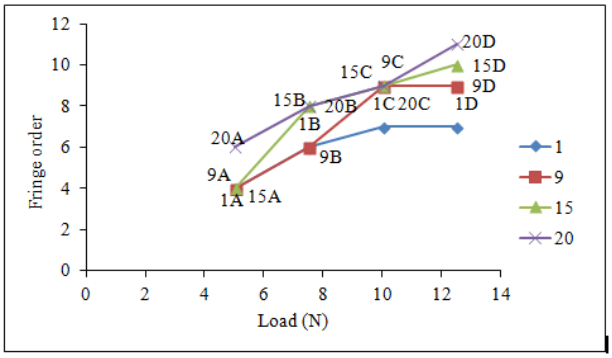

Figure 6: Counted fringe order graph with optical magnification 1x, 9x, 15x and 20x based on increasing load.

From Figure 6, it can be seen increasing of average fringe order with 9x optical magnification:

$$\overline{\Delta N}_{9x} = \frac{(9_A - 1_A)+(9_B - 1_B)+(9_C - 1_C)+(9_D - 1_D)}{n}$$

The average addition of fringe order can be observed for 15x magnification expressed as:

$$\overline{\Delta N}_{9x} = \frac{(15_A - 1_A) + (15_B - 1_B) + (15_C - 1_C) + (15_D - 1_D)}{n}$$

where n = number of data and data = number of loading level = 4

$$\overline{\Delta N}_{15x} = \frac{(4-4) + (8-6) + (9-7) + (10-7)}{4}$$

$$\frac{7}{4} = 1.75$$

The average addition of fringe order can be observed for 20x magnification expressed as:

$$\overline{\Delta N}_{20x} = \frac{(20_A - 1_A) + (20_B - 1_B) + (20_C - 1_C) + (20_D - 1_D)}{n}$$

where n = number of data and data = number of loading level = 4

$$\overline{\Delta N}_{20x} = \frac{(6-4) + (8-6) + (9-7) + (11-7)}{4}$$

$$= \frac{10}{4} = 2.5$$

From the three calculations above, it can be seen there is an increasing trend for the extra magnitude of the average fringe order obtained by increasing the optical zoom level.
Similarly, with 15x optical magnification, average fringe order is 1.75 and with 20x optical magnification, its value is 2.5.

The experimental result and numerical analysis comparison are shown in Figure 7.

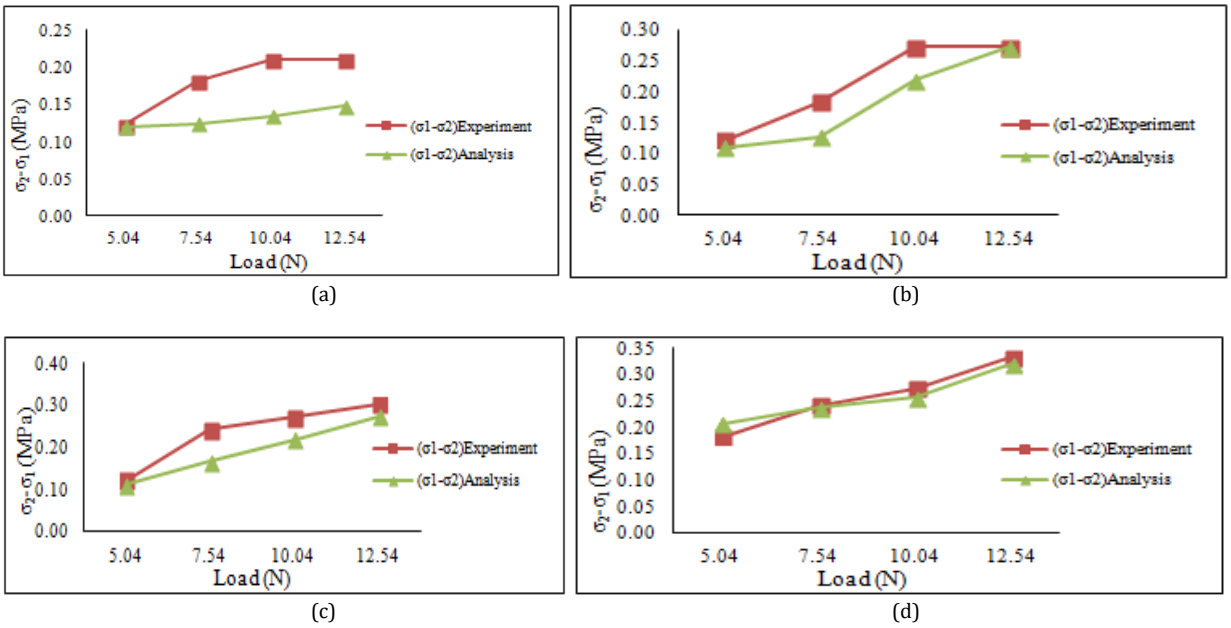

Figure 7: The comparison graph with 1x (a), 9x (b), 15x (c), and 20x (d) optical magnification

Figure 7 (a) shows the major strain differences obtained from the experimental and the major strain differences obtained from the analysis are different. From figure 7 (b) it can be observed that the difference of the principal strain obtained from the experiments and the difference of the principal strain obtained from the analysis had similar shape even though the space of both curves was large enough. Almost all of the points of the loading of the curve of the experimental principal strain difference lied on top of analysis curve. However, it can't be concluded that both curves are correlated.

Figure 7 (c) shows the experimental curve of principal strain difference lied on top of the analysis curve at any load. At the lower load, it indicates that both curves have a trend to coincide at one point. However, in the range of load from 7.54 to 10.04, the difference of the curves is large enough so that it can be concluded that at 15x optical magnification, there was no correlation between the results of experiment and analysis.

Based on Figure 7 (d), it can be observed the difference of the principal strain obtained from experimental lied on top of the difference of the principal strain obtained from analysis using finite element software at the load above 7.54 N. Results differed when the load was reduced from 7.54 N where experimental curve lied under analysis curve.

Therefore, the difference of both curves is small enough so that it can be concluded the experimental and analysis result at 20x magnification was similar. In short, there is a correlation between experimental result and numerical analysis at 20x magnification. From Figure 7, percentage of average error of experimental result compared with numerical analysis can also be calculated i.e. 37.34 % for 1x magnification, 19.73% for 9x magnification, 22.60% for 15x magnification and 5.87% for 20x magnification.

4. CONCLUSION

This study has shown an alternative method in determining fringe order by combining monochromatic lighting, magnifying object and image processing using the photoelasticity method. The experimental result using four optical magnification strength was compared with numerical analysis result. It was concluded there is an increasing trend of average additional fringe with increased optical magnification. A maximum increasing of average additional fringe was 2 at 20x optical magnification compared with the original size of the specimen. Percentage of average error of experimental result compared with numerical analysis showed a tendency to decrease with increasing optical magnification. The bigger the magnification, the greater the correlation between experimental result and numerical analysis.

ACKNOWLEDGEMENT

This research was supported by Independent Superior Fund Program Sepuluh Nopember (ITS) Institute Technology, Surabaya, 2011. The authors also acknowledge the financial support provided by Politeknik Negeri Medan, Medan, Indonesia. The authors express their gratitude to

Dr. Arridina Susan Silitonga, S.T., M. Eng for her assistance in improving this paper.

REFERENCES

[1] Ayatollahi, M., Mirsayar, M., Dehghany, M. 2011. Experimental determination of stress field parameters in bi-material notches using photoelasticity. Materials & Design, 32, 4901.

[2] Zakeri, M., Ayatollahi, M., Guagliano, M. 2011. A photoelastic study of T-stress in centrally cracked Brazilian disc specimen under mode II loading. Strain, 47, 268.

[3] Lee, J.I., Lee, Y., Kim, N.Y., Kim, Y.L., Cho, H.W. 2013. A Photoelastic Stress Analysis of Screw-and Cement-Retained Implant Prostheses with Marginal Gaps. Clinical implant dentistry and related research, 15, 735.

[4] Patil, P., Vyasarayani, C., Ramji, M. 2017. Linear least squares approach for evaluating crack tip fracture parameters using isochromatic and isoclinic data from digital photoelasticity. Optics and Lasers in Engineering, 93, 182.

[5] Karalekas, D., Agelopoulos, A. 2006. On the use of stereolithography built photoelastic models for stress analysis investigations. Materials & design, 27, 100.

[6] Jannotti, P., Subhash, G., Ifju, P., Kreski, P.K., Varshneya, A.K. 2011. Photoelastic Measurement of High Stress Profiles in Ion-Exchanged Glass. International Journal of Applied Glass Science, 2, 275.

[7] Dubey, V.N., Grewal, G.S. 2009. Noise removal in three-fringe photoelasticity by median filtering. Optics and Lasers in Engineering, 47, 1226.

[8] Kihara, T. 2006. A Measurement Method for Birefringent Plate using Elliptically Polarized Light. Strain, 42, 255.

[9] Ju, Y., Ren, Z., Wang, L., Mao, L., Chiang, F.P. 2018. Photoelastic method to quantitatively visualise the evolution of whole-field stress in 3D printed models subject to continuous loading processes. Optics and Lasers in Engineering, 100, 248.

[10] Ajovalasit, A., Petrucci, G., Scafidi, M. 2015. Review of RGB photoelasticity. Optics and Lasers in Engineering, 68, 58.

[11] Chang, C., Lien, H., Lin, J. 2008. Determination of reflection photoelasticity fringes analysis with digital image-discrete processing. Measurement, 41, 862.

[12] Kasimayan, T., Ramesh, K. 2010. Digital reflection photoelasticity using conventional reflection polariscope. Experimental Techniques, 34, 45.

[13] Lei, Z., Yun, H., Zhao, Y., Xing, Y., Pan, X. 2009. Study of shear transfer in Al/epoxy joint by digital photoelasticity. Optics and Lasers in Engineering, 47, 701.

[14] Liu, X., Dai, S. 2015. Mathematical Morphology Guided Automatic Unwrapping Isoclinic Phase Map in White Light Photoelasticity. Journal of the Optical Society of Korea, 19, 643.

[15] Ramji, M., Ramesh, K. 2010. Adaptive Quality Guided Phase Unwrapping Algorithm for Whole-Field Digital Photoelastic Parameter Estimation of Complex Models. Strain, 46, 184.

[16] Tamrakar, D., Ramesh, K. 2002. Noise-free Determination of Isochromatic Fringe Order by Load Stepping. Strain, 38, 11.

[17] Yao, X.F., Jian, L.H., Xu, W., Jin, G.C., Yeh, H.Y. 2005. Digital shifting photoelasticity with optical enlarged unwrapping technology for local stress measurement. Optics & Laser Technology, 37, 582.

[18] Madhu, K.R., Ramesh, K. 2007. Noise removal in three-fringe photoelasticity by adaptive colour difference estimation. Optics and lasers in Engineering, 45, 175.

[19] Marsavina, L., Craciun, E.M., Tomlinson, R.A. 2008. Combining thermo-photo elasticity for analysis of cracked bodies Journal of Optoelectronics and Advanced Materials, 10, 2876

[20] Dally, J.W., Riley, W.F. 1991. Optical methods of stress analysis